Optimizing the numerical port for inverted microstrip gap waveguide in full-wave simulators

Optimizing the Numerical Port for Inverted Microstrip Gap Waveguide in Full-Wave Simulators

Jinlin Liu[1], Ashraf Uz Zaman[1], and Per-Simon Kildal[1]
[1]Department of Signals and Systems, Chalmers University of Technology, Gothenburg, Sweden, jinlin.liu@chalmers.se

***Abstract*—Currently the inverted microstrip gap waveguide has been considered as a promising technology for millimeter wave wireless applications. Theoretically, the new structure may be considered as a two layer shielded structure where the bottom layer consists of an array of periodic metallic pins which works as an artificial magnetic conductor (AMC). However, it is difficult to evaluate electromagnetic properties and performance of the new waveguide by using traditional waveguide ports or discrete ports in available full-wave simulator. In order to solve the problem, this paper proposes an effective method to determine dimensions of traditional waveguide ports in existing commercial full wave simulator to be used while simulating the inverted microstrip gap waveguide structures. The procedure includes the analysis of quasi-TEM mode of the inverted microstrip gap waveguide and the corresponding size of the waveguide port, as well as the location and boundary conditions used in the simulation software. The numerical port proposed in this work is much better than the ports used previously.**

I. Introduction

Recently, a new topology of waveguide technology was proposed in [1-2] and validated in [3-4] for high frequency microwave applications, referred to as gap waveguides. Compared with hollow rectangular waveguides and microstrip lines, the gap waveguide presents some advantages. Hollow rectangular waveguide usually suffers from the problem of poor electrical contacts when it is manufactured in two split blocks or metal blocks. On the other hand, microstrip lines suffer from increasing dielectric losses at higher frequency and spurious resonance when it is encapsulated or packaged. Gap waveguide provides very low loss and high quality factor even for millimeter waves [5], and also offers proper RF packaging and mechanical shielding [6-10] characteristics. Thus, the gap waveguide is an appropriate technological solution above 30 GHz. The gap waveguide technology exists in four different major realizations so far: the groove, ridge, inverted microstrip gap waveguide [1] and the microstrip-ridge gap waveguide [9]. The present paper deals with inverted microstrip gap waveguide shown in Fig. 1. Based on the research of soft- and hard-surfaces, the structure can be treated as an oversized parallel plate waveguide between a smooth and a high impedance surface layer. In such a way it creates a parallel-plate stopband over a specific frequency range. The dispersion diagram for such a stopband structure is shown in Fig. 2. The waves can thereby be guided in directions where the texture is smooth, such as along grooves, ridges or metal strips [1]. The large stopband allows a quasi-TEM mode to propagate in the air gap above the metal strip. This fact implies that the quasi-TEM mode of the inverted microstrip

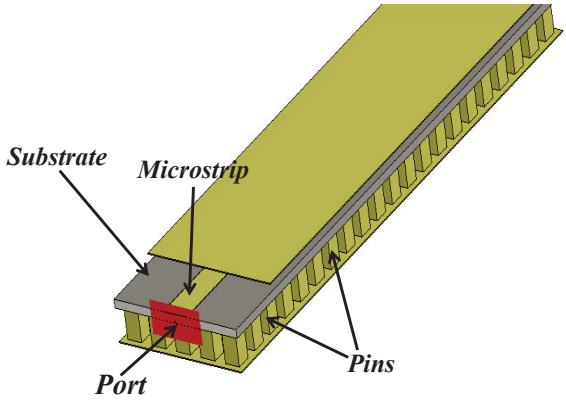

(a)

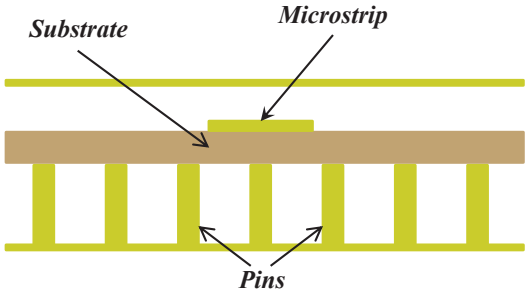

(b)

Fig. 1. Geometrical configuration of inverted microstrip gap waveguide. (a) 3-D view for inverted microstrip gap waveguide. (b) Cross-sectional view for inverted microstrip gap waveguide.

gap waveguide can be utilized for microwave and millimeter wave circuits. So far there are some direct applications of gap waveguide technology in the antenna field [11-14]. The numerical design of gap waveguide circuits and antennas is usually complicated because the existing simulation tools do not supply any suitable port to simulate the influence of wave propagation on textured metallic pins structures. In this paper we will improve the existing numerical waveguide ports proposed in [15] by determining new dimensions and locations of the waveguide ports relative to the pins structure, in such a way that the reflections at the port become lower than in [15].

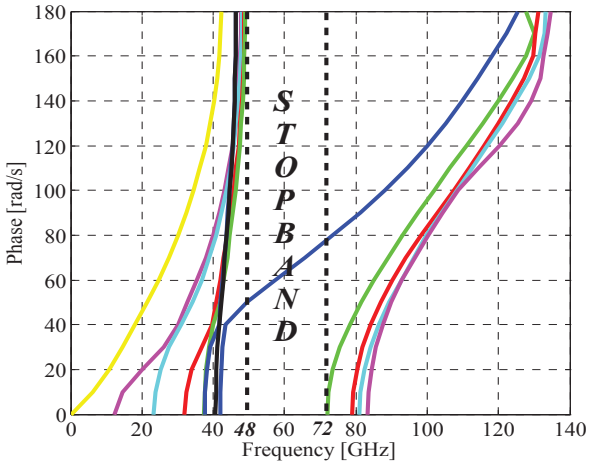

Fig. 2. Dispersion diagram for inverted microstrip gap waveguide and the blue curve crossing over the stopband represents the quasi-TEM mode.

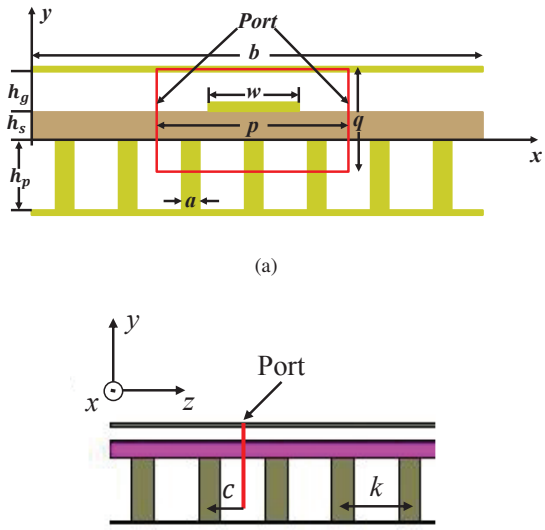

(a)

(b)

Fig. 3. Geometrical configuration of inverted microstrip gap waveguide. (a) Front-view for inverted microstrip gap waveguide. (b) Side-view for inverted microstrip gap waveguide.

II. THE WAVEGUIDE PORT DETAILS FOR INVERTED MICROSTRIP GAP WAVEGUIDE

In full-wave EM simulators the discrete ports and waveguide ports are widely applied for analyzing ordinary hollow rectangular waveguide and microstrip circuits. However, such ports are not suitable for gap waveguide components. The analyzed geometry of inverted microstrip gap waveguide and corresponding rectangular waveguide port are shown in Fig. 3. We use a so-called PMC shielded rectangular waveguide port, which means that the port is in an opening PMC plate. In order to determine the width and the height of the PMC shielded port, we have applied numerical methods. Concretely, we have analyzed a large number of inverted microstrip gap waveguide models with different widths of metal strips and thereafter obtained the electromagnetic energy distribution in the air gap along the lateral (x) direction. The corresponding numerical port must theoretically cover the cross section of the quasi-TEM wave and extend in x-direction up to p which is then given by

$$p = 3w \tag{1}$$

More exactly, we choose the port dimension in the lateral (x) direction to be

$$\frac{b-3w}{2} \leq p \leq \frac{b+3w}{2} \tag{2}$$

Let us now return to solve the vertical dimension of the port. As described, the surface of the metal pins structure at $y = h_p$ can be theoretically treated as a PMC surface. The E- and H-fields inside the PMC are zero, but not within an artificial PMC like the one we have. Here we have utilized the EM simulator to determine the electromagnetic energy distribution in the pin regions. Fig. 4 illustrates the corresponding cross-sectional electric field distribution of inverted microstrip gap waveguide, which helps us to determine the vertical dimension q of the port. As shown in Fig. 4, the electromagnetic field attenuates in vertical direction (y) and q assumed to be given as

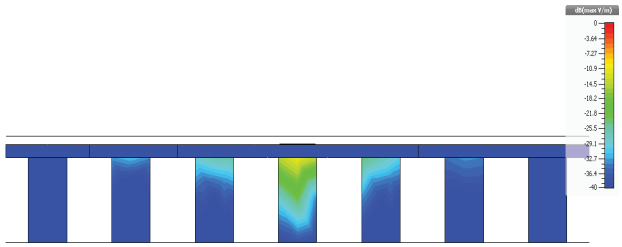

Fig. 4. Normalized electromagnetic energy distribution in textured metallic pins structure.

$$q = h_g + h_s + dh_p \tag{3}$$

where d is the ratio of the lower port extension to the entire pin height. For inverted microstrip gap waveguide in this paper d is defined as $0.5 \leq d \leq 0.65$. Moreover, the port position in longitudinal direction (z) should be considered as well. As shown in Fig. 3(b), the gap waveguide can take periodic forms of metallic pins and air. In the case of metal, all E- and H-fields components must be zero inside the conducting region. Thereby, the port in longitudinal direction (z) is merely configured in the air between pins. The optimized numerical results show that the longitudinal (z) position of port is in the middle of periodicity ($c = \frac{k}{2}$). In addition, in our case

the mode domain of the port is not electrically shielded, such as for instance in a coaxial waveguide. Therefore, we must activate a special treatment of the boundary. In our present work the boundary of the waveguide port is treated as a PMC shielded frame. In the following section we compare the traditional electric port introduced in [15] with the PMC shielded port. And the numerical simulations by full wave EM simulator show very good agreements with the forementioned theory. Consequently, this kind of port can be widely used for design microwave circuits based on inverted microstrip gap waveguide technology in the future.

III. Numerical Models and Numerical Simulations

In the following section we will simulate a straight inverted microstrip gap waveguide, a T-junction power divider and 1:4 microwave power divider based on the inverted microstrip gap waveguide, by using the different port models.

A. Simulation of Straight Inverted Microstrip Gap Waveguide

Firstly, Fig. 5 shows the detailed schematic of the straight inverted microstrip gap waveguide:

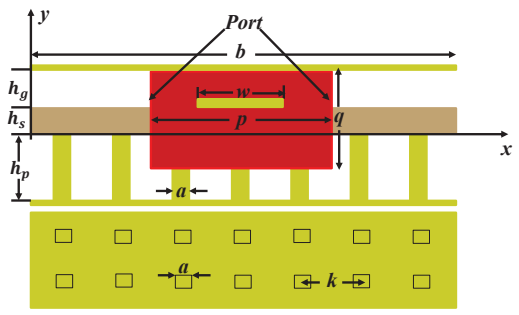

(a)

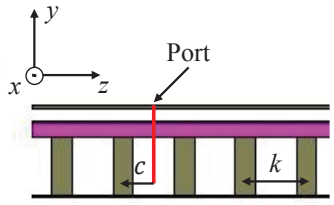

(b)

Fig. 5. Geometrical configuration of inverted microstrip gap waveguide. (a) 3-D view for inverted microstrip gap waveguide. (b) Side-view for inverted microstrip gap waveguide.

Substrate Material	Rogers 4003 (ε^*=3.55)
Thickness of Substrate [h_s]	0.225 mm
Thickness of Air Gap [h_g]	0.25 mm
Width of Microstrip [w]	1.25 mm
Width of Metallic Pin [a]	0.5 mm
Width of Gap Waveguide [b]	7 mm
Periodicity of Pin [k]	1.25 mm
Height of Pin [h_p]	1 mm
Port Position of Pin [c]	0.625 mm

The length l of inverted microstrip gap waveguide model is 26.5 mm. Fig. 6 shows the simulated reflection coefficient S_{11} of straight inverted microstrip gap waveguide based on geometrical parameters mentioned above. Here we have carried out the sweep parameter method to analyze reflection coefficient S_{11}. The approach is that the width of waveguide port is fixed at the optimized value $3w$ and its height varies from 0 to 0.65 mm. The results in Fig. 6 show that the dimension of waveguide port at $d = 0.55$ minimize the pin effect on inverted microstrip gap waveguide. In the same way, Fig. 7 illustrates the optimized lateral dimension of waveguide port. As long as the lateral dimension of the waveguide port is bigger than $3w$ most of the energy in the electromagnetic field will be covered by the waveguide port.

A preliminary research of characteristic impedance of

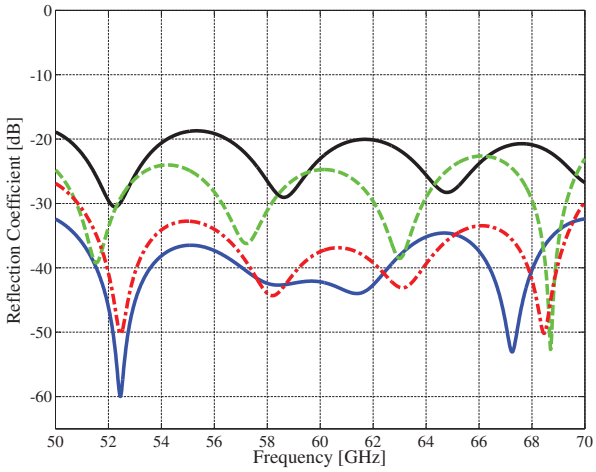

Fig. 6. Reflection coefficient for different port geometries. $p = 3w$ = 3.3 mm. q varies in size from 0 to 0.65. **Black**: d = 0. **Green**: d = 0.3. **Red**: d = 0.65. **Blue**: d = 0.55.

inverted microstrip gap waveguide was done by utilizing a regular waveguide port in [15]. Fig. 8 shows the reflection coefficient parameter S_{11} obtained both by using a regular waveguide port approach in [15] and the optimized port introduced in this work. The results show that the new numerical waveguide port with PMC shielding produces about -10 dB lower reflection compared to the approach presented in [15]. Thus the new port will improve the numerical accuracy of full wave simulations on inverted microstrip gap waveguide structures.

B. T-Junction Power Divider and 1:4 Distribution Networks

In the next part, we will introduce the PMC shielded ports when designing a T-junction power divider and a simple 1:4 distribution networks based on the inverted microstrip gap waveguide technology. And the results of reflection coefficients S_{11} will be compared with the ports introduced in [15]. Fig. 9 shows the complete structure of the T-junction power divider based on the inverted microstrip gap waveguide.

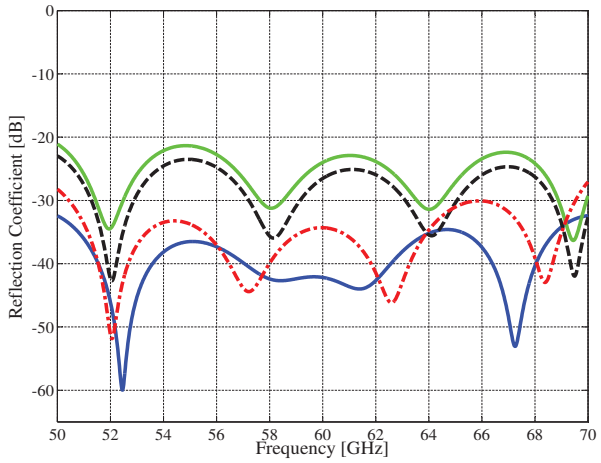

Fig. 7. Reflection coefficient for different port geometries. q = 0.55 mm. p varies in size from 1.25 to 4. **Green**: p = 1.5 mm. **Black**: p = 2 mm. **Red**: p = 3 mm. **Blue**: p = 3.5 mm.

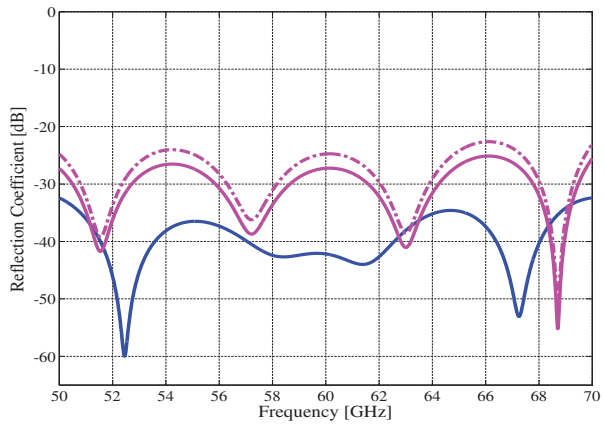

Fig. 8. Comparison of reflection coefficients using a regular waveguide port and PMC-shielding port. **Pink Dashed Line**: Regular Waveguide Port p = 3.5 mm; d = 0. **Pink Solid Line**: Regular Waveguide Port p = 3.5 mm; d = 0.55. **Blue Dashed Line**: PMC shielded Port p = 3.5 mm; d = 0.55.

The working frequency band of the component is from 50 to 70 GHz. Fig. 10 shows the reflection coefficients based on both a normal waveguide port and PMC shielded port. The results show that the new PMC shielded port produces the 4 dB lower S_{11} than the approach presented in [15]. In practice the distribution networks based on inverted microstrip gap waveguide is more complicated than a single T-junction power divider. Therefore, we will here numerically analyze and compare normal waveguide port and the PMC shielded port for a simple 1:4 power divider distribution networks, as shown in Fig. 11. The working frequency band is from 54 to 68 GHz. Fig. 12 shows the reflection coefficients based on both using normal waveguide ports and PMC shielded ports. The results proves that for this case the PMC shielded ports produces the 3 dB lower S_{11} than approach presented in [15].

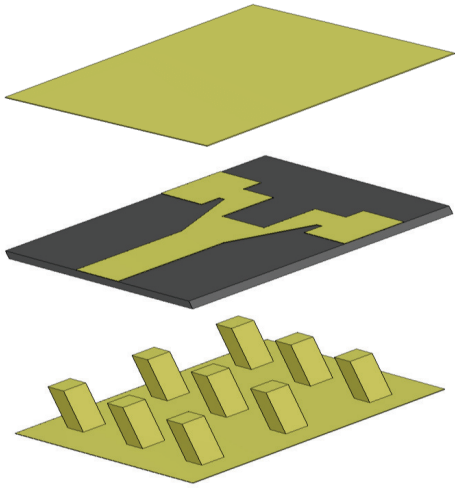

Fig. 9. 3-D view for a single T-junction power divider based on inverted microstrip gap waveguide.

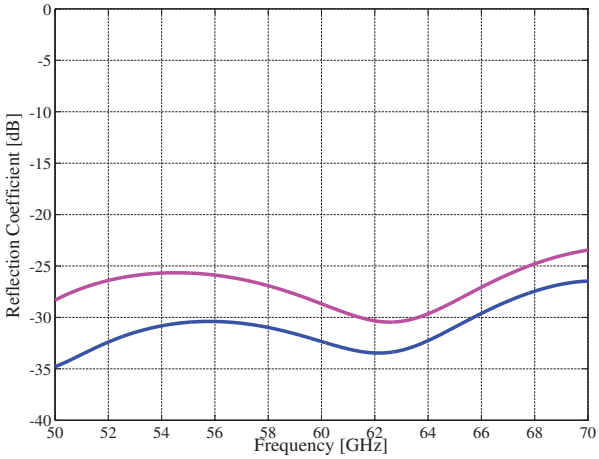

Fig. 10. Comparison of reflection coefficients using a regular waveguide port and PMC shielded port for a single T-junction power divider. **Pink Solid Line**: Regular Waveguide Port introduced in [15]. **Blue Solid Line**: PMC shielded Port.

IV. Conclusion

We have presented a numerical port study for inverted microstrip gap waveguide. An optimized gap waveguide port has been proposed to minimize the effect of the periodicity of the pins on the simulations of the inverted microstrip gap waveguide. The numerical simulations of straight inverted microstrip gap waveguide show that by choosing the correct dimensions for the port, it is possible to minimize the reflection and S_{11} becomes better than -35 dB for a back to back configuration. This means, the reflection due to a single port is even

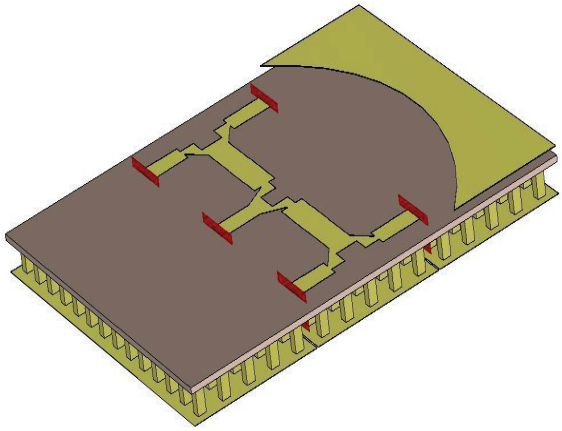

Fig. 11. 3-D view for a simple 1 : 4 distribution networks based on inverted microstrip gap waveguide.

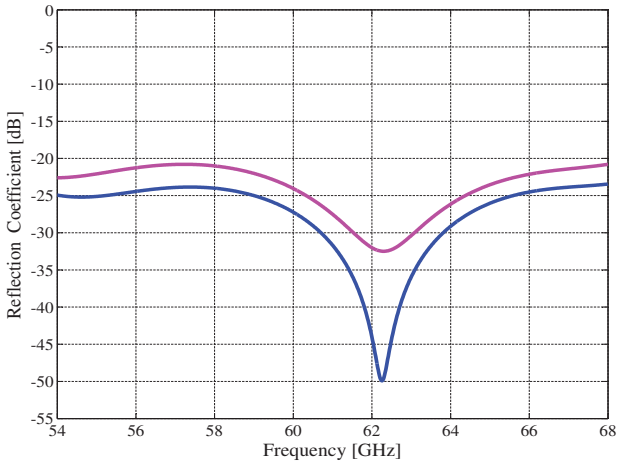

Fig. 12. Comparison of reflection coefficients using a regular waveguide port and PMC shielded port for a simple 1 : 4 distribution networks based on inverted microstrip gap waveguide. **Pink Solid Line**: Regular Waveguide Port introduced in [15]. **Blue Solid Line**: PMC shielded Port.

lower and should be -41 dB which is good enough to simulate most passive microwave components based on this type of gap waveguide structures. Furthermore, we have applied the novel PMC shielded port for simulating a simple T-junction power divider and a 1:4 power divider distribution network based on inverted microstrip gap waveguide. The numerical results of both structures show that the novel PMC shielded port has obviously improved reflection coefficients and this new kind of PMC shielded port will be beneficial when designing microwave circuits based on inverted microstrip gap waveguide.

REFERENCES

[1] P.-S. Kildal, "Three metamaterial-based gap waveguides between parallel metal plates for mm/submm waves", *3rd European Conference on Antennas and Propagation EUCAP* 2009, Berlin, Germany, March 23-27, 2009.

[2] P.-S. Kildal, E. Alfonso, A. Valero, and E. Rajo, "Local metamaterial-based waveguides in gaps between parallel metal plates ", *IEEE Antennas and Propagation Letters,* vol. 8, pp. 84-87, 2009.

[3] P.-S. Kildal, A. Uz. Zaman, and Eva. Rajo, E. Alfonso, A. Valero. Nogueira, "Design and Experimental Verifacation of Ridge Gap Waveguide in Bed of Nails for parallel Plate Mode Suppression", *IET Microwave Antennas and Propagation,* vol. 5, no. 3, pp. 262-270, March 2011.

[4] A. U. Zaman, P.-S. Kildal, M. Ferndahl, and A. Kishk, "Validation of ridge gap waveguide performance using in-house TRL calibration kit,"in *4th European Conference on Antennas and Propagation EUCAP* 2010, Barcelona, Spain, 12-16 April, 2010.

[5] E. A. Alos, A. U. Zaman, P.-S. Kildal, "Ka-Band Gap Waveguide Coupled-Resonator Filter for Radio Link Diplexer Application ", *IEEE Transactions on Components, Packaging and Manufacturing Technology,* vol. 3, no. 5, pp. 870-879, May 2013.

[6] Eva. Rajo, A. Uz. Zaman, P.-S. Kildal, "Parallel plate cavity mode suppresion in microstrip circuits packages using a lid of nails", *IEEE Microwave and Wireless Components Letters,* vol. 20, no. 1, pp. 31-33, Dec. 2009.

[7] A. Uz. Zaman, J. Yang, P.-S. Kildal, "Using Lid of Pins for packageing of Microstrip Board for Descrambling the Ports of Eleven Antenna for Radio Telescope Applications", *IEEE international Symposium on Antennas and Propagation* 2010, Toronto, Canada, July 11-17, 2010.

[8] E. Rajo-Iglesias, P. S. Kildal, A. U. Zaman, and A. Kishk, "Bed of Springs for Packaging of Microstrip Circuits in the Microwave Frequency Range ", *IEEE Transaction on Components, Packaging and Manufacturing Technology,* vol. 2, no. 10, pp. 1623-1628, Oct. 2012.

[9] A. Algaba. Brazalez, A. Uz. Zaman, P.-S. Kildal, "Improved Microstrip Filters Using PMC Packaging by Lid of Nails ", *IEEE Transaction on Components, Packaging and Manufacturing Technology,* vol. 2, no. 7, pp. 1075-1084, July, 2012.

[10] Zaman, A.U., Alexanderson, M., Vukusic, T, "Gap Waveguide PMC Packaging for Improved Isolation of Circuit Components in HighFrequency Microwave Modules", *IEEE Transactions on Components, Packaging, and Manufacturing Technology,* vol. 4, no. 1, pp. 16-25, Jan. 2014.

[11] Zaman, A.U., Kildal, P.-S. "Wide-Band Slot Antenna Arrays With Single-Layer Corporate-Feed Network in Ridge Gap Waveguide Technology", *IEEE Transactions on Antennas and Propagation,* vol. 62, no. 6, pp. 2992-3001, June, 2014.

[12] Zaman, A.U., Kildal, P.-S. "Slot antenna in ridge gap waveguide technology ", *6th European Conference on Antennas and Propagation EUCAP*, 2012, Prague, Czech, 26-30 March, 2012.

[13] Seyed Ali Razavi, P.-S. Kildal, Liangliang Xiang, Esperanza Alfonso Alos and Haiguang Chen, "2×2-slot Element for 60GHz Planar Array Antenna Realized on Two Doubled-sided PCBs Using SIW Cavity and EBG-type Soft Surface fed by Microstrip-Ridge Gap Waveguide", *IEEE Transactions on Antennas and Propagation,* vol. 62, no. 9, September. 2014

[14] Pucci, E. , Rajo-Iglesias, E. , Vazquez-Roy, "Planar Dual-Mode Horn Array with Corporate-Feed Network in Inverted Microstrip Gap Waveguide", *IEEE Transactions on Antennas and Propagation,* vol. 62, no. 7, pp. 3534 - 3542, July, 2014.

[15] Hasan Raza, Jian Yang, Per-Simon Kildal, "Study of the Characteristic Impedance of Gap Waveguide Microstrip Line realized with Square Metal Pins", *7th European Conference on Antennas and Propagation EUCAP*, 2013, Gothenburg, Sweden, 8-12 April, 2013.